Bioresource Technology Reports 32 (2025) 102416

Contents lists available at ScienceDirect

Bioresource Technology Reports

journal homepage: www.sciencedirect.com/journal/bioresource-technology-reports

Comparative analysis of microbial communities in biofilm-associated microplastic in river, seawater, anaerobic sludge, and soil environments

Kavya Sunil [a], Dicky John Davis G [a,*]

[a] Department of Bioinformatics, Sri Ramachandra Institute of Higher Education and Research, Porur, Chennai, Tamil Nadu, 600116, India

ARTICLE INFO

Keywords:
Microplastics
Plastisphere
Metatranscriptomics
Plastic-degrading enzymes
Microbial diversity
Biodegradation

ABSTRACT

Microplastics (MPs) form biofilms called the "plastisphere," hosting diverse microbial communities. This study compared microbial communities using metatranscriptomic data from 40 biosamples of eight different types of plastic (PVC, PLA, PHA, PBS, PBAT, PS, PP, and POM) of biofilm-related microplastics found in river, seawater, soil, and anaerobic sludge environments. Proteobacteria and Thaumarchaeota are the most common phyla, while Nitrososphaera, Gammaproteobacteria, and Alphaproteobacteria are important classes, according to MetaPhlAn taxonomic profiling. Microplastics in rivers and seawater were more diverse than those in soil, based on alpha diversity measures (Shannon Index ~2.44–2.70; Simpson Index ~0.09–0.19). The composition of communities in different environments varied significantly according to the Bray Curtis beta diversity test. Functional profiling using DIAMOND alignment against PlasticDB enzyme sequences produced high-confidence (>50 %) hits for polyhydroxyalkanoate/polyhydroxybutyrate depolymerases, alkane hydroxylase, lipase, hydrolase, nylon hydrolase, 3-hydroxyvalerate dehydrogenase, and other plastic-degrading enzymes. Some of these were linked to the breakdown of butanoate and caprolactam through pathway reconstruction. Key enzyme producers like *Pseudomonas species, Escherichia coli, Acidovorax, Ralstonia, and Alcanivorax* remained consistent across environments, and the nylon breakdown pathway was fully expressed in marine samples. This metatranscriptomic analysis highlights the taxonomic composition, diversity, and plastic-degrading potential of plastisphere communities, providing insights into their environmental distribution and supporting microbial-driven bioremediation strategies.

1. Introduction

1.1. Microplastics and biofilms

Microplastics (MPs), defined as plastic particles smaller than 5 mm, have emerged as pervasive environmental pollutants, posing significant threats to ecosystems and human health due to their persistence and widespread distribution, making their interaction with biofilms a critical research focus (Sun et al., 2023). These particles, originating from the fragmentation of larger plastics, industrial activities, and consumer products, accumulate in marine, freshwater, and terrestrial environments, where they serve as substrates for microbial colonization, leading to the formation of biofilms complex communities of microorganisms embedded in extracellular polymeric substances (EPS), often termed the "plastisphere" (Yang et al., 2021). Biofilms modify the physical and chemical elements of MP. The physical structure of MPs undergo changes because of biofilms through enhanced buoyancy and sorption dynamics and environmental reactions that can be further explained by supporting biological processes (Ventura et al., 2024). The biofilm enables multiple environmental processes including pollutant adsorption along with vertical transport and possible biodegradation, underscores their ecological significance (Jiao et al., 2024). MPs encompass various polymers, including polyethylene (PE), polypropylene (PP), polystyrene (PS), polyvinyl chloride (PVC), polyethylene terephthalate (PET), polylactic acid (PLA), polyhydroxyalkanoates (PHA), polybutylene succinate (PBS), polybutylene adipate terephthalate (PBAT), and polyoxymethylene (POM), each hosting diverse microbial assemblages (Tu et al., 2020).

In marine environments, biofilms on PE and PP exhibit bacteria and fungi that alter plastic properties, while freshwater systems show higher microbial diversity on PVC and PS compared to surrounding water, and biodegradable plastics like PLA and PHA support denser biofilm formation (Odobel et al., 2021; Du et al., 2022). Soil biofilms on PBAT and PBS influence microbial activity and carbon cycling, though degradation

* Corresponding author.
E-mail address: dicky@sriramachandra.edu.in (D.J. Davis G).

https://doi.org/10.1016/j.biteb.2025.102416
Received 9 June 2025; Received in revised form 17 September 2025; Accepted 8 November 2025
Available online 11 November 2025

is slower than in aquatic systems (Sun et al., 2022; Wang et al., 2025; Kim et al., 2024).

Microbial biofilms produce enzymes such as esterases, urethanases, cutinases, laccases, proteases, amylases, PHA depolymerases, monooxygenases, and hydrolases, which break down complex polymer structures, with genes like *petH* in *Ideonella sakaiensis* for PET hydrolysis, *lac* in *Pseudomonas* for PE oxidation, *phaZ* in *Bacillus* for PHA degradation, *est* in *Actinobacteria* for PLA, and *alkB* in *Alcanivorax* for PP, driving these processes (Mohanan et al., 2020). Despite their importance, biofilms amplify ecotoxicological risks by acting as vectors for harmful contaminants and pathogens, enhancing the sorption of heavy metals and persistent organic pollutants, increasing their bioavailability and transfer through food webs, and potentially contributing to greenhouse gas emissions like methane and carbon dioxide during MP mineralization (Mishra et al., 2024,Bocci et al., 2024). A significant research gap exists in comprehensively elucidating the microbial mechanisms and environmental factors governing biofilm-mediated MP degradation across diverse ecosystems, as the efficiency and scalability of degradation by bacteria and fungi, which form robust biofilms, remain poorly understood (Zahid et al., 2024).

Evidence from freshwater systems suggests that biofilm composition varies with environmental conditions, such as salinity and nutrient availability, yet the specific metabolic pathways driving degradation are underexplored (Sun et al., 2023; Chen et al., 2020). In marine environments, plastic-degrading microorganisms within biofilms contribute to surface erosion, but their effectiveness under natural conditions is unclear (Kumar et al., 2020). Another gap lies in the limited understanding of MP-biofilm interactions in soil environments, where factors like soil texture and organic matter influence microbial activity, and soil plastispheres affect carbon cycling and contaminant transport, yet field-based studies are scarce (Wang et al., 2024a, 2024b). Supporting evidence shows that soil biofilms on PBAT and PBS involve *Rhizobium* and *Burkholderia* facilitating biodegradation via metabolic cooperation, while marine POM biofilms exhibit microbial colonization linked to surface weathering, with *Archaea* potentially aiding degradation in deep-sea conditions (Morohoshi et al., 2018). In local contexts, such as urban rivers and coastal regions, the accumulation of microplastics highlights the need for mitigation strategies.

This study investigates the microbial composition of biofilms on MPs in river, marine, soil, and anaerobic sludge environments, characterizes the functional pathways involved in their degradation, and analyse diversity of different environment, aiming to provide a comparative analysis of microbial communities across these matrices to deepen understanding of their ecological roles and inform strategies for mitigating MP pollution.

2. Materials and methods

2.1. Data collection from NCBI-SRA

40 transcriptomic samples were analysed in this study; all sourced from the NCBI-SRA (Sequence Read Archive) database. Selection was based on the availability of detailed metadata, sufficient sequencing depth, and explicit association with microplastic biofilms. These data were derived from four distinct types of investigations, each representing different environments, such as Sea water (PRJNA902427), River water (PRJNA714465), Anaerobic sludge (PRJNA1098580), and Soil (PRJNA1146720) from China. The BioProject accession number PRJNA902427 from the Sea water environment contained 32 biosamples in total, of which we used only 2 biosamples for this study. The metatranscriptomic sequence was performed using the Illumina NovaSeq 6000 platform. Similarly, we took only 9 of the 45 biosamples of metatranscriptomic sequence performed on the Illumina HiSeq 2500 platform from the river environment (PRJNA714465), 2 of the 8 biosamples from the anaerobic sludge environment (PRJNA1098580) were metatranscriptomic samples performed on the Illumina NovaSeq 6000 platform, and 27 of the 27 biosamples from the soil environment (PRJNA1146720) were samples of metatranscriptomic sequence performed on the Illumina NovaSeq 6000 platform. (Table 1).

2.2. Data analysis

Analysis of data processed through Galaxy India Software (https://india.usegalaxy.eu/) platform. The analysis process requires all its necessary tools through this platform. Steps such as Quality Control, assembly, taxonomic profiling along with visualization processes and pathway analysis and enzyme identification (Galaxy Community, 2024).

2.3. Data preprocessing and assembly

The analysis software FastQC and Cutadapt was used to assess the quality of 40 raw sequence reads from all samples. Cutadapt processed the data to ensure accuracy and reliability of the results. Read assembly was performed using the MEGAHIT tool.

2.4. Taxonomic profiling

A metagenomic examination of assembled sequence data was performed using MetaPhlAn. Through metagenomic marker genes MetaPhlAn produced outcomes that showed microbial taxa together with their quantitative distributions for each sample.

2.5. Visualization

MetaPhlAn generated results underwent visual presentation with Krona as well as GraPhlAn software. Krona generates pictures showing microbial taxonomic distributions in samples while GraPhlAn provides additional detailed information concerning the taxonomic structure. The taxonomic structure achieves better detail and interconnected features through this method.

2.6. Alpha and Beta diversity analysis

Microbial diversity was assessed using beta diversity analysis based on Bray-Curtis distance, calculated with the Vegan package in R to examine differences between communities. Alpha diversity in each environment was measured using both Shannon and Simpson indices, calculated with Python's Scikit-bio package. Species presence counts could also be accessed through Scikit-bio. Alpha diversity results were visualized as boxplots generated in R using the ggplot2 package to compare diversity indices across environments.

2.7. Multivariate analysis

To further explore differences in microbial community structure,

Table 1
lists the metatranscriptomic datasets used in this study, including the study title, sequencing platform, sampling location, and corresponding references, all retrieved from the NCBI Sequence Read Archive (SRA).

Title of the study	Platform	Biosample	Location	Reference
Metatranscriptome of biofilm microplastic in **Seawater**	Illumina (Novaseq 6000)	2	China	Peng Qin et al., 2023
Metatranscriptome of bacterial community in **River** water	Illumina Hiseq 2500	9	China	Xiaojian Wu et al., 2022
Field experiment of microplastic – **Soil** metatranscriptome	Illumina (Novaseq 6000)	27	China	Wang et al., 2024a
Viral metatranscriptome sequencing of **Sludge** pvc	Illumina (Novaseq 6000)	2	China	Bei Zang et al., 2024

multivariate ordination methods were applied. Principal Coordinates Analysis (PCoA) was performed on the Bray-Curtis dissimilarity matrix to reduce the data into two dimensions and highlight clustering patterns. Non-metric Multidimensional Scaling (nMDS) was also conducted using the Vegan package in R, which preserves the rank order of distances and is widely used for ecological data. In addition, a Permutational Multivariate Analysis of Variance (PERMANOVA) was carried out using the adonis2 function in Vegan with 999 permutations to test the statistical significance of community differences among environments. All ordination results were visualized using ggplot2.

2.8. Gene prediction

Assembled reads from MEGAHIT were analysed for potential genes using the PRODIGAL gene prediction tool in Galaxy, which produced both nucleotide and protein translation files for further analysis.

2.9. Enzyme identification

To identify enzymes responsible for plastic degradation, sequence data of relevant enzymes were retrieved from PlasticDB, comprising a total of 228 protein sequences. Alignment was performed using the DIAMOND BLAST tool with the gene protein files generated by PRODIGAL and the PlasticDB sequences to identify hits and positive matches.

3. Pathway analysis

The pathway was analysed using the enzyme result that matched the gene sequence for more than 50 %. BRENDA enzyme database was used for potential organisms and pathways responsible for degradation. Other databases, including the KEGG and METACYC enzyme and pathway databases, were used to build additional enzyme pathways. HUMAnN tool from galaxy was also used to find presence/absence and abundance of microbial pathways.

4. Results

4.1. Quality control

Every sequence read was subjected to FastQC and MultiQC, and none received a low-quality rating. Cutadapt was used to trim the reads that required the adapter sequence to be trimmed. Following quality control, the Megahit assembly generated a well-assembled read file output.

4.2. Taxonomic profiling and abundance

Regardless of the environment, the most common phyla in all samples were Proteobacteria, followed by Thaumarchaeota, according to the taxonomic profiling of the sequence reads using MetaPhlAn. Gamma-, Beta-, Alphaproteobacteria, and Nitrososphaera were the most common classes in the phylum Proteobacteria and Thaumarchaeota, respectively. Hydrogenophilalia, Alphaproteobacteria, Flavobacteriia, Actinomycetes, Thermoleophilia, and Oligoflexia were among the other low-abundance classes. Other phyla that were also found in low abundance included Actinobacteria, Bacteroidota, Planctomycetes, Firmicutes, and Cyanobacteria. The most frequently occurring species among the samples, accompanied by their percentage abundances are listed in Table 2. Apart from the highest abundance species, there are other significant species that were present in low abundance, such as *Alcanivorax nanhaiticus, Alteromonas* sp., *Phaeobacter italicus, Moraxella osloensis, Pseudomonas* sp., *Ralstonia pickettii, Pseudoalteromonas* sp. in seawater microplastics; *Sphaerotilus natans, Bacteroides graminisolvens, Azotobacter* sp., *Pseudomonas* sp., *Rhizobium* sp., etc. in river samples irrespective of the plastic type; *Pseudomonas cremoris, Hydrogenophilus thermoluteolus, Comamonas denitrificans, Sphingomonas* sp. in soil samples irrespective of the plastic type; and *Phyllobacterium calauticae,*

Table 2
The most commonly detected species across the samples, along with their corresponding relative abundance percentages.

Environment	Sample	Species	Relative abundance
Sea Water	M scale Microplastic	*Qipengyuania aquimaris*	14.5234
	MM scale Microplastic	*Streptococcus salivarius*	2.5550
River Water	PVC3	*Azohydromonas lata*	2.7547
	PVC2	*Azonexus hydrophilus*	2.1465
	PVC1	*Azohydromonas lata*	3.3479
	PLA3	*Azohydromonas lata*	3.0444
	PLA2	*Azohydromonas lata*	2.7347
	PLA1	*Azohydromonas lata*	3.3362
	Water 3	*Azonexus hydrophilus*	1.6933
	Water 2	*Azonexus hydrophilus*	1.4262
	Water 1	*Azonexus hydrophilus*	1.6005
Soil	PHA3	*Nitrososphaerales*	0.5472
	PHA2	*Nitrososphaerales*	73.4579
	PHA1	*unclassified.*	84.2554
	PBS3	*Nitrososphaerales*	1.4645
	PBS2	*Escherichia coli*	8.2062
	PBS1	*Escherichia coli*	3.3871
	PBAT3	*Escherichia coli*	5.52565
	PBAT2	*Microcoleus*	0.1016
	PBAT1		
	PVC3	*Buchnera aphidicola*	0.07739
	PVC2	*Nitrososphaerales*	0.2637
	PVC1	*Escherichia coli*	7.7513
	PS3	*unclassified*	49.418
	PS2	*Nitrososphaerales archaeon*	22.628
	PS1	*Escherichia coli*	41.1033
	PP3	*Escherichia coli*	65.345
	PP2	*Escherichia coli*	49.1921
	PP1	*Nitrososphaerales*	33.976
	POM3	*Escherichia coli*	39.618
	POM2	*Escherichia coli*	30.269
	POM1	*Escherichia coli*	52.846
	PLA3	*Escherichia coli*	34.475
	PLA2	*Nitrososphaerales*	50.1530
	PLA1	*Nitrososphaerales*	73.4579
	CK3	*unclassified,*	78.498
	CK2	*unclassified*	46.144
	CK1	*Escherichia coli*	42.856
Anaerobic Sludge	20 PVC	*Pedobacter cryoconitis*	54.0860
	0 PVC	*Pedobacter cryoconitis*	48.3327

Escherichia coli, Ralstonia pickettii, Acinetobacter, Pseudomonas fluorescens in the anaerobic sludge environment. The relative abundance of dominant microbial phyla across various environments is shown in Fig. 1.

4.3. Visualization

The GraPhlAn and Krona tool's phylogenetic visualization made the relationships between the identified taxa very evident. GraPhlAn phylogenetic tree of sample 1 (M-SCALE MP from seawater), highlighting the distribution of Alcanivoracaceae (green) and Roseobacteraceae (blue) families in a seawater environment is shown in Fig. 2 and Krona pie chart visualization of sample 1 is shown in Fig. 3.

4.4. Alpha and beta diversity results

The alpha diversity analysis of the samples using Shannon and Simpson metrics by Python (scikit-bio) revealed varying amounts of diversity between each sample. A low Simpson index (which is closer to zero) and a high Shannon Index indicate the sample had high diversity, which is species richness and even distribution of species, where as a high Simpson index (which is closer to one) and a low Shannon index indicate the sample has low diversity. Alpha diversity results across environments were compared using boxplots of Shannon and Simpson

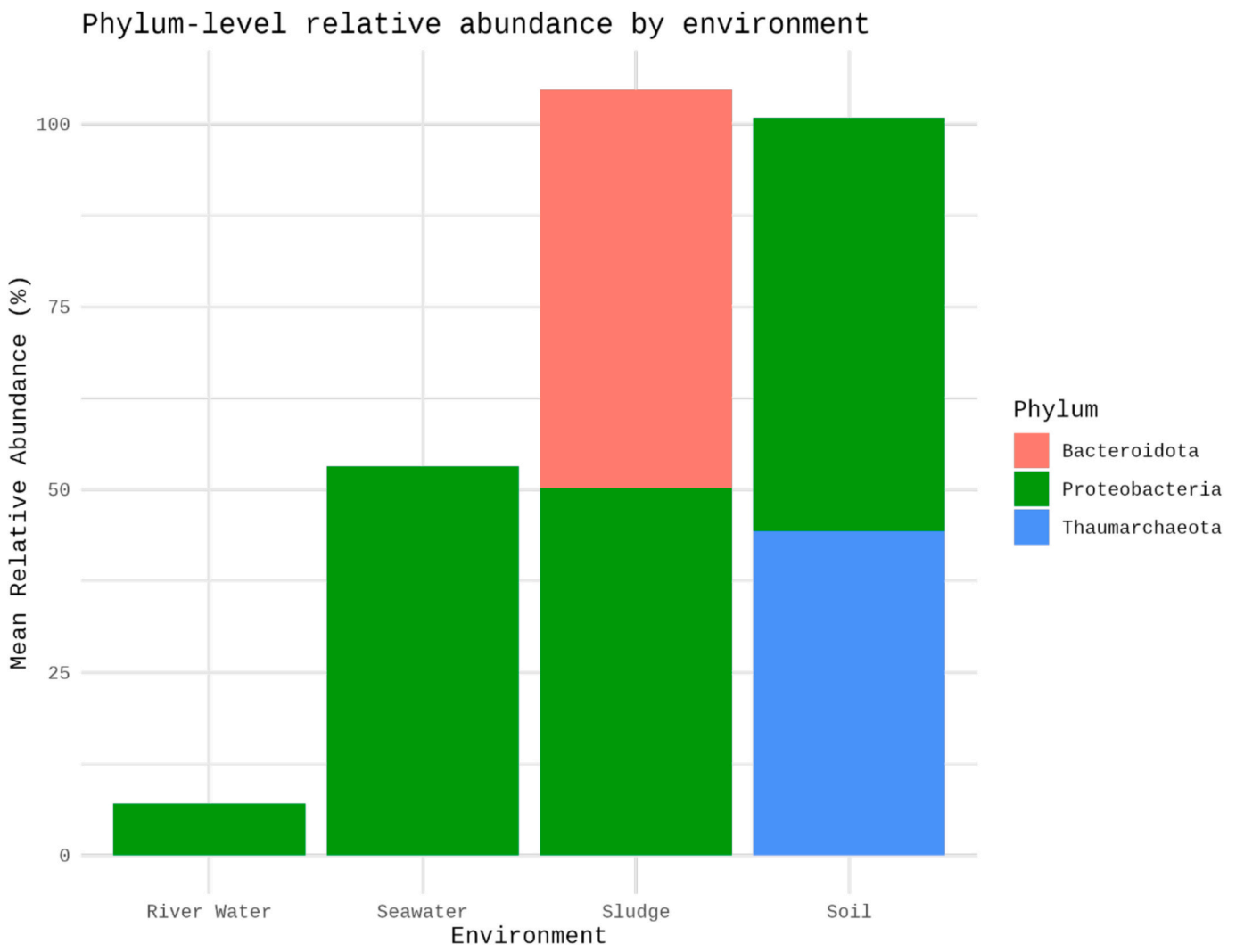

Fig. 1. Relative abundance of dominant microbial phyla across environments. Bar plots show the distribution of microbial communities in river water, seawater, sludge, and soil samples. Proteobacteria were consistently dominant across all environments, with sludge showing high representation of both Proteobacteria and Bacteriodota, while soil exhibited notable contributions from Proteobacteria and Thaumarchaeota.

indices, shown in Figs. 4 and 5, respectively.

The boxplots offer a clear visual representation of the Shannon and Simpson index distributions across the sample types river water, seawater, sludge, and soil. For the Shannon index, river water and seawater display higher median values, approximately 2.70 and 2.44 respectively, with tight interquartile ranges (IQRs) and few outliers, suggesting a stable and consistently high diversity. The sludge sample has a median Shannon value around 1, with a slightly broader IQR, indicating moderate diversity with some variation. The soil sample, however, shows a lower median Shannon value ranging from 0.3 to 1.80, accompanied by a wider IQR and several outliers, highlighting significant variability and generally reduced diversity, especially in cases like PVC and PBAT where the index drops to 0, indicating no diversity. Regarding the Simpson index, river water and seawater exhibit low median values, around 0.09 to 0.19, with narrow IQRs, reinforcing their high species evenness and richness. Sludge has a median Simpson value near 0.5 with a wider IQR, showing more variability, while soil presents a higher median value between 0.3 and 1, with a broad IQR and outliers, reflecting low diversity and instances of single-species dominance, such as in PVC and PBAT samples where the index reaches 1.

In this study, microplastics from sea and river environments, such as PVC and PLA, showed high species richness and evenness (D ~ 0.09 – 0.19) and Shannon index (~ 2.70–2.44), while microplastics from soil, such as PHA, PBS, PS, PP, POM, and PLA (D ~ 0.3–1) and Shannon Index (~ 1.80–0.3), showed very low diversity. PVC and PBAT from soil showed no diversity and were dominated by only one species (D = 1) and Shannon Index (0).

The Bray-Curtis method of beta diversity analysis using R (Vegan) examined the differences between the communities of organisms in various samples. Most of the samples displayed a high Bray-Curtis distance, which is near one, while only a small number of samples displayed a low Bray-Curtis distance.

4.5. *Multivariate analysis*

The PCoA plot based on the Bray-Curtis dissimilarity matrix demonstrates that microbial communities are primarily grouped by environment as shown in Fig. 6. River water (red) and seawater (green) samples exhibit considerable dispersion across the plot, with river water showing a broad distribution and seawater forming a few scattered points, suggesting diverse microbial compositions rather than a tight clustering. Soil samples (purple) are distinctly clustered in the lower right quadrant, indicating a high degree of similarity among them. The first principal coordinate (PCoA1, 39.7 % variance) effectively separates water samples (left/upper) from soil samples (right), while the second principal coordinate (PCoA2, 15.3 % variance) contributes additional

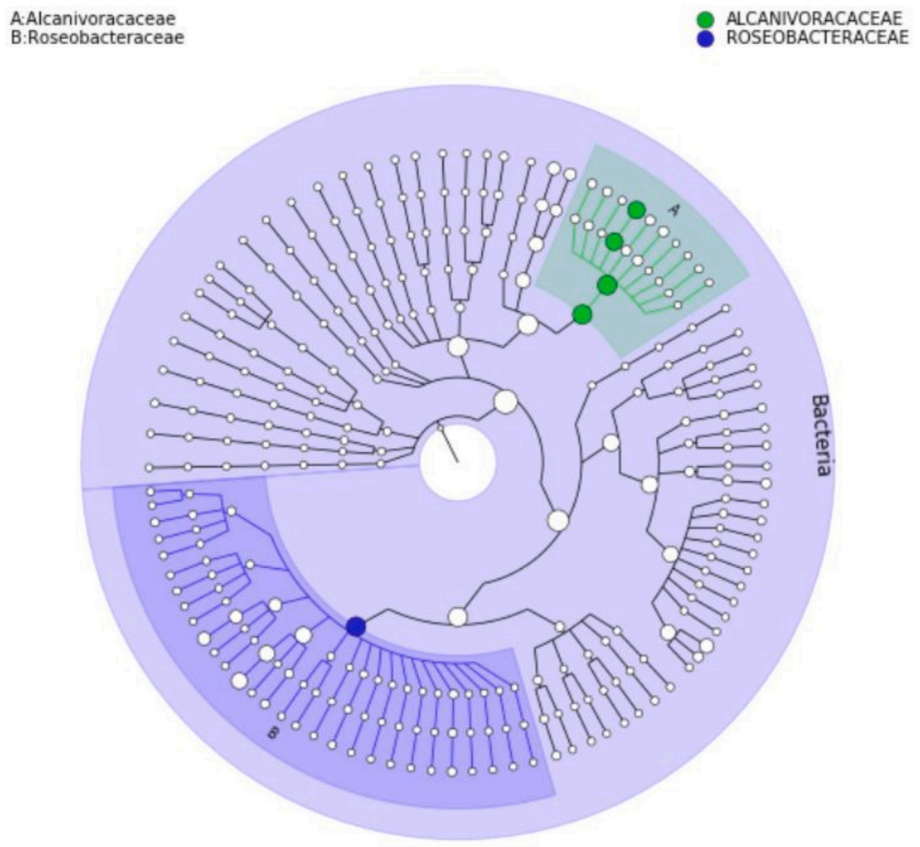

Fig. 2. GraPhlAn phylogenetic tree of sample 1 (M-SCALE MP from seawater), highlighting the distribution of Alcanivoracaceae (green) and Roseobacteraceae (blue) families in a sea environment. This phylogenetic tree illustrates the taxonomic relationships within sample 1. The tree highlights two specific bacterial families, emphasizing their relative abundance and phylogenetic positions. The circular layout, generated using GraPhlAn, provides a clear visualization of microbial diversity and family-level clustering in the sampled marine ecosystem. (For interpretation of the references to colour in this figure legend, the reader is referred to the web version of this article.)

spread.

The nMDS ordination based on the Bray–Curtis dissimilarity matrix indicates that microbial community composition is largely shaped by the environment as shown in Fig. 7. River water samples (red) are broadly scattered across the upper right and central portions of the plot, suggesting high heterogeneity among them. Seawater samples (green) are less frequent and more dispersed, with one distinct outlier positioned in the upper left, pointing to unique microbial assemblages. Sludge samples (cyan) form a tight cluster near the origin, reflecting strong compositional similarity. Soil samples (purple), which represent the largest group, display a looser distribution concentrated in the central to lower right regions, indicating moderate similarity but with some internal variation. Along NMDS1, samples are separated primarily along a left-to-right gradient, while NMDS2 contributes additional vertical spread. However, interpretation remains tentative in the absence of a reported stress value to evaluate the robustness of the ordination.

A PERMANOVA test (adonis function) was conducted to statistically evaluate differences between groups. The analysis showed that environment explained a significant portion of the variation in community structure ($R^2 = 0.384$, $F = 7.49$, $p = 0.001$) The results are summarized in Table 3. This indicates that approximately 38 % of the variability in microbial diversity can be attributed to environmental differences, while the remaining 62 % is accounted for by other unexplained factors. These results are consistent with the observed clustering in the ordination plots, where distinct separation of communities according to environmental categories was evident.

4.6. Pathway analysis

The gene predicted from the assembled read produced potential genes that may function because of the organisms present. This gene file, in conjunction with the PlasticDB enzyme sequence that is responsible for the degradation of plastic, was aligned using diamond blast, and the enzymes that were found to have more than 50 % of hits with the predicted gene sequence were 3 HV dehydrogenase, Laccase, PHA depolymerase, PEG dehydrogenase, PHB depolymerase, Protease, PEG aldehyde dehydrogenase, Carboxylesterase, Copper oxidase, Polyesterase, PETase, Polyamidase, Copper oxidase, Polyesterase, PETase, Lipase, 3HB oligomer hydrolase, Alkane monooxygenase, Esterase, Hydrolase, Nitrobenzyl Esterase, Nylon hydrolase, MHETase, and PBS depolymerase.

Microplastic samples from seawater demonstrated 100 % hit rates for the enzymes nylon hydrolase, nylon oligomer degrading enzyme, and nylon hydrolase responsible for nylon degradation. The organisms that produce these enzymes were retrieved from Brenda database and the metabolic pathway from Kegg and Metacyc. *Pseudomonas* spp. and *Escherichia coli* known to produce these enzymes were found in both samples. The enzyme is responsible for Caprolactam degradation and nylon-6 oligomer degradation. The pathway involves several key enzymes and genes which may be produced by *Pseudomonas spp* including Nylon hydrolases such as: 6-aminohexanoate cyclic dimer hydrolase (nylA), 6-aminohexanoate oligomer hydrolase (nylB), 6-aminohexanoate oligomer endohydrolase (nylC). The degradation proceeds via conversion of nylon-6 polymers to 6-aminohexanoate and ultimately to adipate, through intermediate steps involving enzymes like

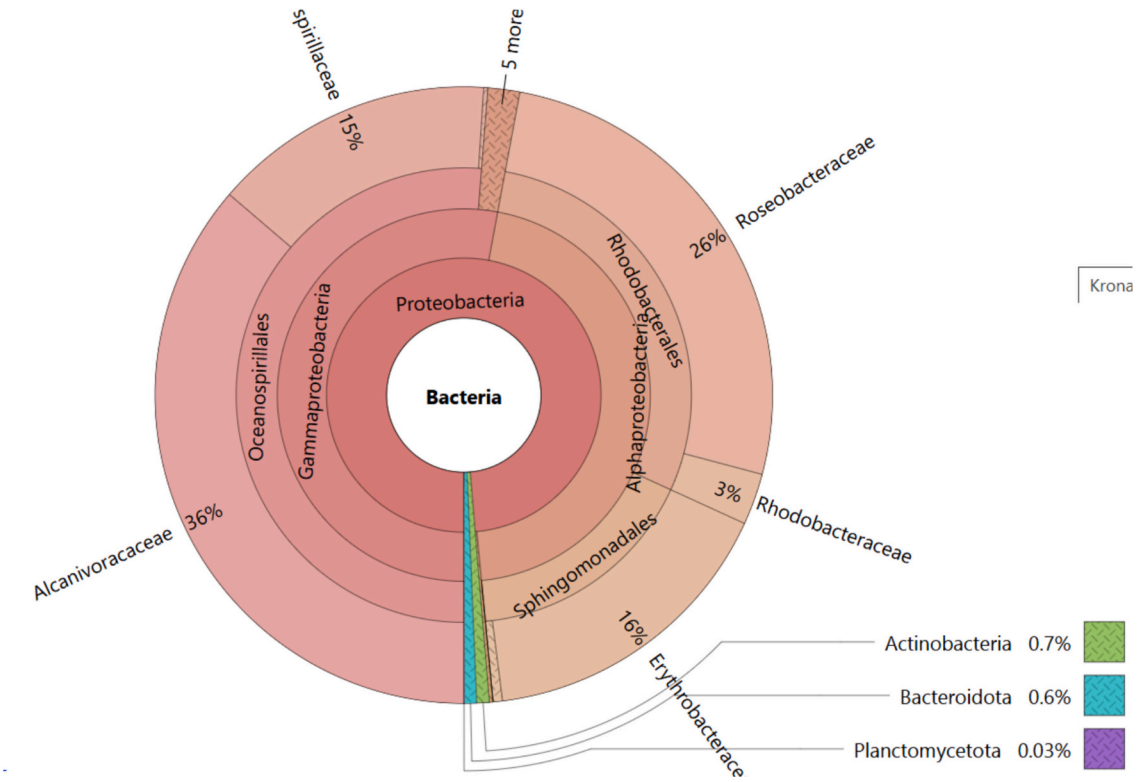

Fig. 3. Krona pie chart visualization of sample 1 (M-SCALE MP from seawater), depicting the microbial community composition at the phylum and family levels. The chart reveals the dominance of Proteobacteria (central ring), with key families such as Alcanivoracaceae (36 %) and Roseobacteraceae (26 %) highlighted. Other notable groups include Sphingomonadales, Erythrobacterace (16 %) and Rhodobacteraceae (3 %), alongside minor contributors like Actinobacteria (0.7 %), Bacteroidota (0.6 %), and Planctomycetota (0.03 %). This Krona chart provides a hierarchical overview of microbial diversity, emphasizing the prevalence of Proteobacteria in the sea sample.

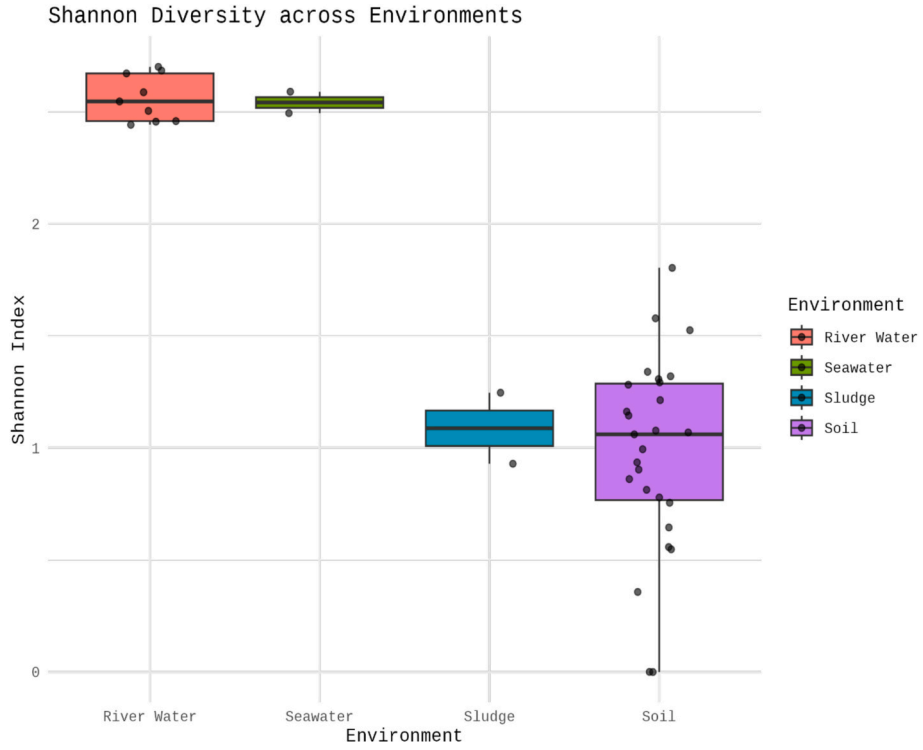

Fig. 4. Alpha diversity (Shannon index) of microbial communities across four environments. Boxplots illustrate the distribution of Shannon diversity values in river water, seawater, sludge, and soil plastisphere samples. River water and seawater exhibited the highest alpha diversity, reflecting greater microbial richness and evenness in aquatic environments, whereas sludge and soil showed comparatively lower diversity, suggesting dominance of specific taxa.

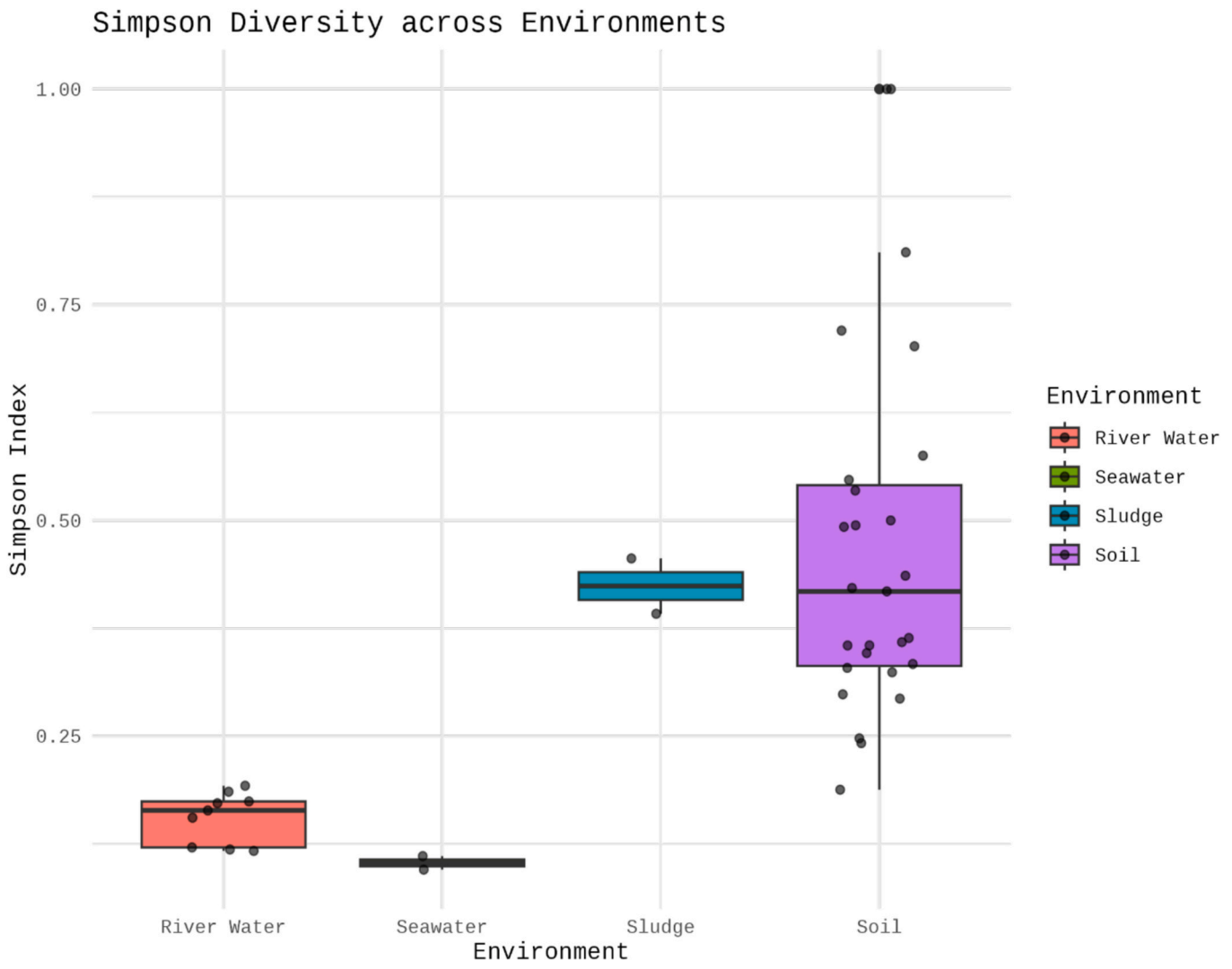

Fig. 5. Alpha diversity (Simpson index) of microbial communities across four environments. Boxplots display the distribution of Simpson diversity values in river water, seawater, sludge, and soil plastisphere samples. River water and seawater showed low dominance with more even communities, whereas sludge and soil reflected higher dominance of specific taxa.

aminotransferases and dehydrogenases. The species like *Arthrobacter*, *Kocuria sp* and *Flavobacterium sp* are also known to produce these enzymes and they were present in river water microplastic such as PVC and PLA but no appropriate sequence hits were found in these samples.

Even though many enzymes displayed more than 50 % hits, only certain enzymes such as 3 HV dehydrogenase, PHA depolymerase, PHB depolymerase, alkane hydroxylase, 3HB oligomer hydrolase, protease, lipase, esterase, hydrolase, and polyurethanase had the proper organisms that produce them. Enzymes such as PHA depolymerase and 3 HV dehydrogenase break down PHA microplastic. Flow chart depicting the initial enzymatic degradation of polyhydroxyalkanoates (PHA) into 3 HV monomers by PHA depolymerase and 3 HV dehydrogenase is shown in Fig. 8 and flow chart illustrating the microbial metabolism of acetoacetate and energy production from microplastic (MP) degradation is shown in Fig. 9. *Pseudomonas* and *Acidovorax sp*, which produce the 3 HV dehydrogenase enzyme, were detected in numerous samples. Only samples from rivers contained *Acidovorax sp*, while samples from all environments contained *Pseudomonas* sp. Although the 3 HV dehydrogenase enzyme was detected in many samples, it was present in over 50 % of the sea water microplastic sample, PVC and PLA sample from the river environment, PP2, POM3, PVC2 from the soil environment, and PVC from anaerobic sludge.

Pseudomonas putida, the enzyme that produces PHA depolymerase, was only detected in river water PVC and PLA samples, even though the enzyme displayed more than 50 % of the hit in many samples. It is known that PHA depolymerase is a part of the butanoate metabolism pathway.

Most of the samples contained PHB depolymerase and 3HB oligomer hydrolase, which are responsible for the degradation of PHB microplastics in the environment. Metabolic pathway of poly(3-hydroxybutyrate) (PHB) microplastic degradation is shown in Fig. 10. In our investigation, we discovered that *Arthrobacter* sp. was present in the PVC and PLA river water sample, *Pseudomonas* sp. was present in all environmental samples, *Ralstonia* sp. was present in the seawater microplastic, POM1 microplastic from soil and PVC microplastic from anaerobic sludge. *Acidovorax* sp. was present in the river water, seawater microplastic, PLA3 from the river, and POM1 from the soil. The enzyme 3HB oligomer hydrolase is produced by a variety of organisms and the metabolic pathway is shown in Fig. 11. *Acidovorax* and *Alcaligenes faecalis* were detected in river water microplastic PVC and PLA, *Pseudomonas* sp. was found in all environmental samples, *Ralstonia* sp. was found in seawater microplastic, POM1 microplastic from soil, and PVC microplastic from anaerobic sludge. It is known that the butanoate metabolism pathway involves both PHB depolymerase and 3HB oligomer hydrolase.

Other enzymes that were present and demonstrated over 50 %

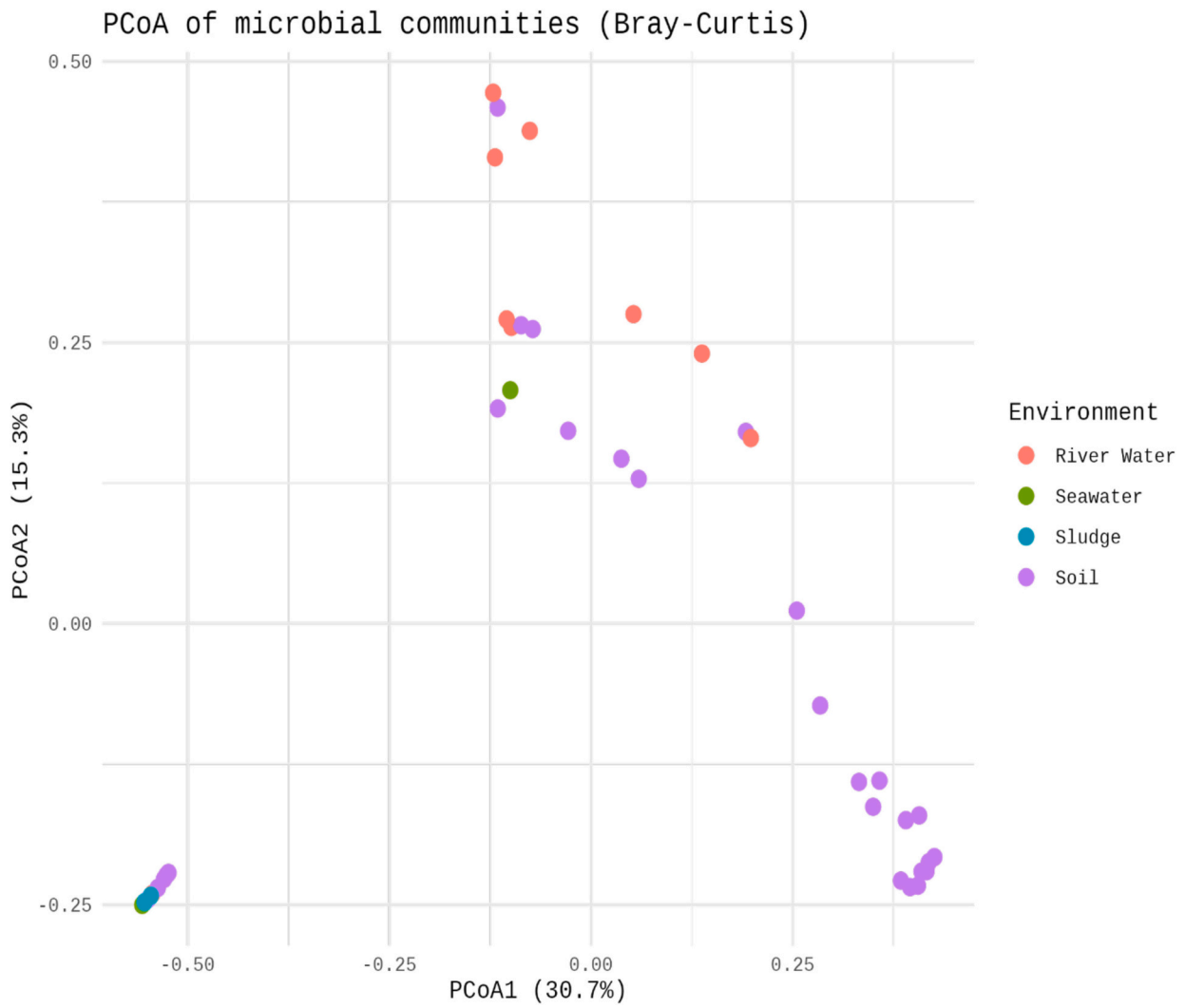

Fig. 6. Principal Coordinates Analysis (PCoA) plot derived from the Bray-Curtis dissimilarity matrix, highlighting the ecological structuring of microbial communities across different environments. River water (red) and seawater (green) samples are characterized by a scattered distribution, suggesting heterogeneity in microbial assemblages, whereas soil samples (purple) exhibit a compact grouping in the lower right, indicative of uniform microbial profiles. (For interpretation of the references to colour in this figure legend, the reader is referred to the web version of this article.)

activity included alkane hydroxylase, protease, lipase, esterase, hydrolase, and polyurethanase; however, the appropriate degradation pathway is unknown. Among these, the degradation pathway mediated by alkane hydroxylase was thoroughly investigated. Primary alcohols (R–CH_2OH) are created in this pathway when alkane hydroxylase (AlkB) first oxidizes microplastics like polystyrene and polyethylene, changing terminal methyl groups (–CH_3) to hydroxyl groups (–OH). Alcohol dehydrogenase (ADH) subsequently reacts with these alcohols, oxidizing them to aldehydes (R–CHO). The enzyme aldehyde dehydrogenase (ALDH) then transforms aldehydes into carboxylic acids (R–COOH). After entering the tricarboxylic acid (TCA) cycle and the β-oxidation pathway, the resultant carboxylic acids undergo additional breakdown into intermediate and energy metabolites. Energy, water (H_2O), and carbon dioxide (CO_2) are the end products of this pathway. *Pseudomonas putida* and *Pseudomonas aeruginosa*, which produce alkane hydroxylase, were detected in PLA and PVC microplastics from rivers; *Pseudomonas fluorescens*, which produces protease, was detected in a PVC sample from anaerobic sludge; *Moraxella* sp., which produces lipase, was detected in PVC and PLA samples from rivers; and *Paenarthrobacter ureafaciens*, which produces hydrolase, was detected in PVC from rivers. *Pseudomonas protegens*, which produces polyurethanase, was discovered in POM1, POM2, and PHA from soil, while the esterase-producing organism *Alcanivorax borkumensis* was discovered in a seawater microplastic sample. The distribution of enzymes with greater than 50 % activity across microplastic samples, as identified through DIAMOND BLAST analysis, notably independent of the presence of corresponding enzyme-producing organisms in the samples shown in Table 4.

The MHETase enzyme which is known to degrade PET microplastic was detected at over 98 % in microplastic PLA and PVC sourced from river water; nevertheless, the organism responsible for its production was absent from the taxonomic profile list generated by Metaphlan.

5. Discussion

Through the metatranscriptomic approach this analysis demonstrated substantial microbial distribution and enzymatic capacity of plastic degradation in four marine environments. The study found strong enzymatic potential which helps microplastic degradation across microbial environments in these four environmental systems: sea and river areas, soil habitat and anaerobic sludge systems.

Both Proteobacteria and Thaumarchaeota phyla emerged as dominant groups in every tested sample. Studies confirm that both Proteobacteria and Thaumarchaeota exist abundantly in microbial communities that associate with plastics because these phyla show high

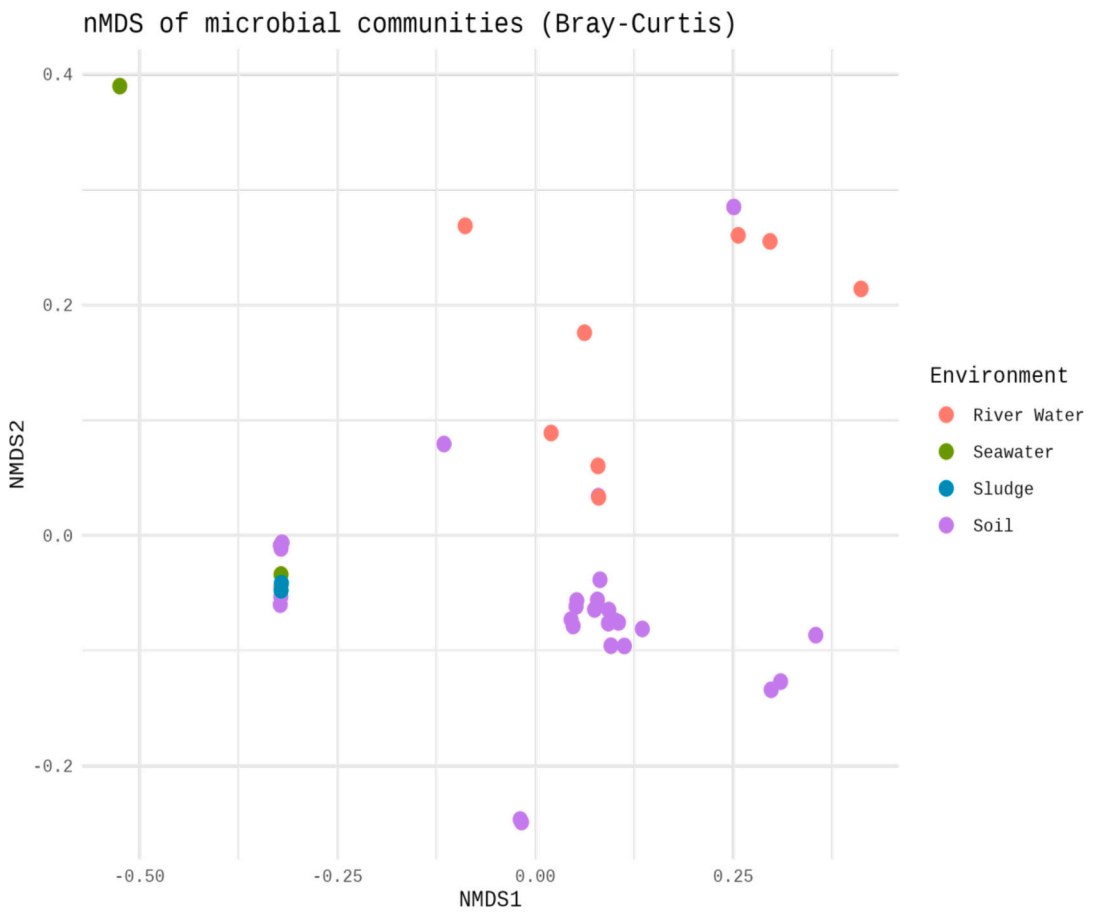

Fig. 7. Non-metric multidimensional scaling (NMDS) plot based on the Bray-Curtis dissimilarity matrix, illustrating the ecological structuring of microbial communities across different environments. River water (red) and seawater (green) samples are broadly dispersed, reflecting variation in community composition, while sludge (cyan) and soil (purple) samples form more compact clusters, indicating greater similarity within these environments. (For interpretation of the references to colour in this figure legend, the reader is referred to the web version of this article.)

Table 3
PERMANOVA results (Bray-Curtis) showing the effect of the environment on microbial community composition. Df, sums of squares, mean squares, F value, R^2, and *p*-values are reported; dashes indicate non-applicable values.

Source	Df	Sums of Squares	Mean Squares	F Value	R^2	Pr (>F)
Environment	3	6.0354	2.0118	7.4873	0.38421	0.001
Residual	36	9.6731	0.2687	–	0.61579	–
Total	39	15.7085	–	–	1.00000	–

Notes: Df = degrees of freedom; sums of squares (SS) and mean squares (MS) calculated for model, residuals, and total; F = F statistic; R^2 = proportion of variance explained; Pr(>F) = *p*-value from 999 permutations. Model Df = 3, residuals = 36, total = 39. Total variation = 15.7085, with 6.0354 explained by the model. MS = 2.0118 (model) and 0.2687 (residuals). F = 7.4873; R^2 = 0.3842 (model), 0.6158 (residuals); Pr(>F) = 0.001, indicating a highly significant effect on the environment.

metabolic flexibility and adaptability to diverse environmental conditions (Vaksmaa et al., 2021; Zettler et al., 2013). Specifically, the prominence of Gamma-, Beta-, and Alphaproteobacteria classes within Proteobacteria, and Nitrososphaera within Thaumarchaeota. The structure and diversity of the plastisphere microbial population varies according to season, location, and plastic substrate type. (Oberbeckmann et al., 2014; Maran and Davis, 2022).

The sea and river microplastic samples which contained PVC and PLA materials showed high species abundance and similar levels of species occurrence. Microplastic samples show opposite diversity patterns with Simpson indices below 0.19 and Shannon indices between 2.44 and 2.70.

The soil samples which contained PHA, PBS, PS, PP, POM and PLA displayed low Simpson indices of 0.3 to 1 in addition to Shannon indices between 0.3 and 1.8. Shannon indices from ~0.3 to 1.8. Different nutrient levels together with environmental conditions appear to cause this difference (Nguyen et al., 2023).

Water ecosystems maintain environmental stability that allows diverse microbial populations to thrive better than selective conditions in soil environments (Gupta et al., 2016; Zheng et al., 2024). The complete dominance of single species in some soil samples, the ecological niche specialization of these microplastics is indicated through complete species dominance characterized by Simpson index = 1 and Shannon index = 0 in samples containing PVC and PBAT.

The microplastic chemical character drives bacterial community development. Beta diversity analysis of microbial communities showed high sample-level dissimilarity patterns when using the Bray-Curtis method since most samples had Bray-Curtis distances near 1. The study demonstrates that microplastic varieties as well as environmental conditions strongly determine the composition of microbial communities since plastic surfaces create separate ecological zones (Li et al., 2021). Low Bray-Curtis distances occurred rarely among microbial communities possibly because of shared plastic types and environmental factors.

The multivariate analyses in this study clearly demonstrate how environmental factors shape the microbial communities on microplastics. The observed clustering and dispersion patterns in the PCoA and nMDS plots suggest that environmental factors are key drivers of

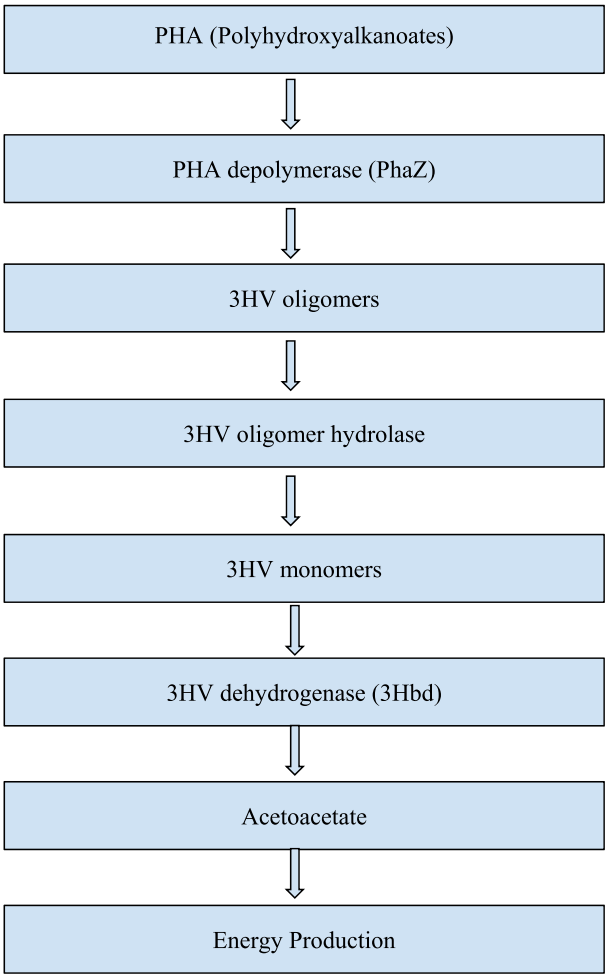

Fig. 8. This figure illustrates the early stages of microplastic (MP) degradation, focusing on the enzymatic breakdown of polyhydroxyalkanoates (PHA). PHA depolymerase (PhaZ) first degrades PHA into 3 HV oligomers, which are further hydrolysed by 3 HV oligomer hydrolase into 3 HV monomers. These monomers are then processed by 3 HV dehydrogenase (3Hbd) to produce acetoacetate, a key intermediate. The flowchart highlights the role of these enzymes in initiating the degradation process within microbial systems, setting the stage for further metabolic processing.

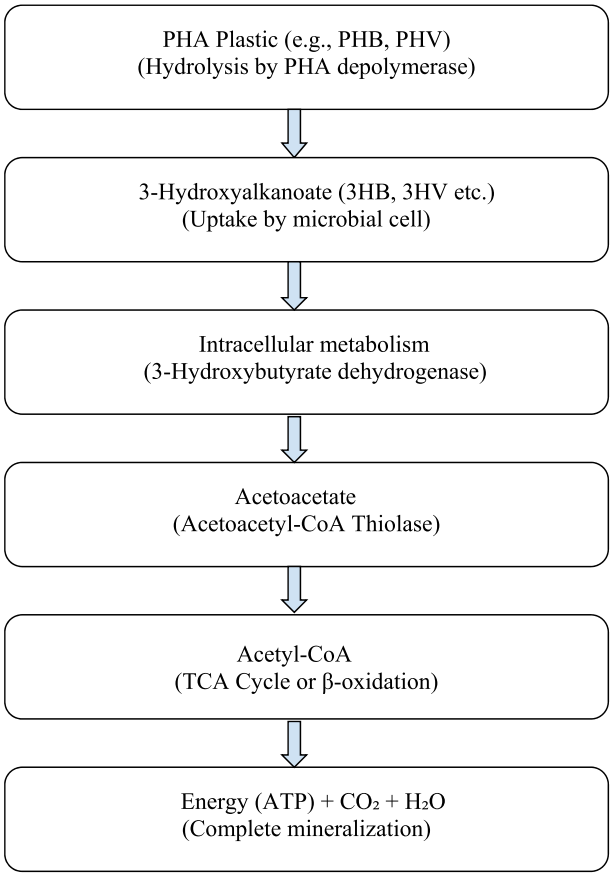

Fig. 9. This figure details the downstream metabolic pathways following the enzymatic breakdown of microplastics (MP). Acetoacetate, produced from 3 HV monomers, is metabolized by microbial cells into acetyl-CoA through the action of acetoacetate-CoA thiolase. Acetyl-CoA then enters the TCA cycle or undergoes β-oxidation, leading to complete mineralization and the production of energy (ATP), CO_2, and H_2O. The flowchart emphasizes the microbial uptake and metabolic processes that convert degradation intermediates into usable energy, completing the MP degradation pathway.

microbial community structure. The broader spread of seawater (green) and river water (red) samples reflects high variability in community composition, likely influenced by fluctuating aquatic conditions, whereas soil (purple) and sludge (cyan) samples form tighter clusters, indicating more uniform assemblages. These patterns align with studies on plastic-colonizing microbes, where MacLean et al. (2021) reported substrate-specific shifts in bacterial diversity between plastics and surrounding soil, highlighting the role of habitat in shaping microbial communities.

PERMANOVA analysis further confirms that environmental variables account for a substantial portion of microbial variation ($R^2 = 0.384$, $F = 7.48$, $p = 0.001$), supporting the interpretation that habitat driven selection is a major determinant of community composition. Similar trends have been reported in aquatic pollution studies, where changes in plastisphere composition were linked to environmental stressors, favoring certain bacterial groups such as Proteobacteria (Malla et al., 2025; Lavanya and Davis, 2023). Likewise, in marine systems, PCoA and PERMANOVA have demonstrated how microplastic characteristics and external environmental factors can increase heterogeneity in plastisphere communities compared to free-living microbes (Zhang et al., 2022).

In mangrove ecosystems, influenced by salinity and tidal dynamics, nMDS and PERMANOVA effectively distinguished plastisphere communities from soil microbiomes with nitrogen-cycling processes potentially contributing to soil clustering (Li et al., 2025). Together, these findings underscore that microbial communities are shaped by both environmental heterogeneity and selective pressures, and that multivariate approaches such as PCoA, NMDS, and PERMANOVA provide complementary insights into ecological structuring across habitats.

These patterns also raise concerns about microplastics as carriers for specialized microbes across ecosystems. In reviews of marine plastic debris, the plastisphere's role in biodegradation and pathogen harbouring has been linked to such structural differences, with multivariate tools like these helping pinpoint ecotoxicological risks (Jacquin et al., 2019). Overall, the findings suggest that aquatic plastispheres might enable faster microbial exchange, while soil ones foster unique adaptations, potentially affecting nutrient cycles or pollutant spread.

Microbial communities showed biodegradation potential through the discovery of enzymes that successfully match over 50 % of the plastic degrading enzyme sequences contained in the PlasticDB database. The environments contained the plastic degrading enzyme set that consisted of 3 HV dehydrogenase and PHA depolymerase together with PHB depolymerase and 3HB oligomer hydrolase, which showed prevalence in PHA and PHB microplastic environments. The butanoate metabolism pathway enzymes arise from *Pseudomonas* spp., *Acidovorax* spp., and *Ralstonia* spp. organisms which persistently existed within the samples

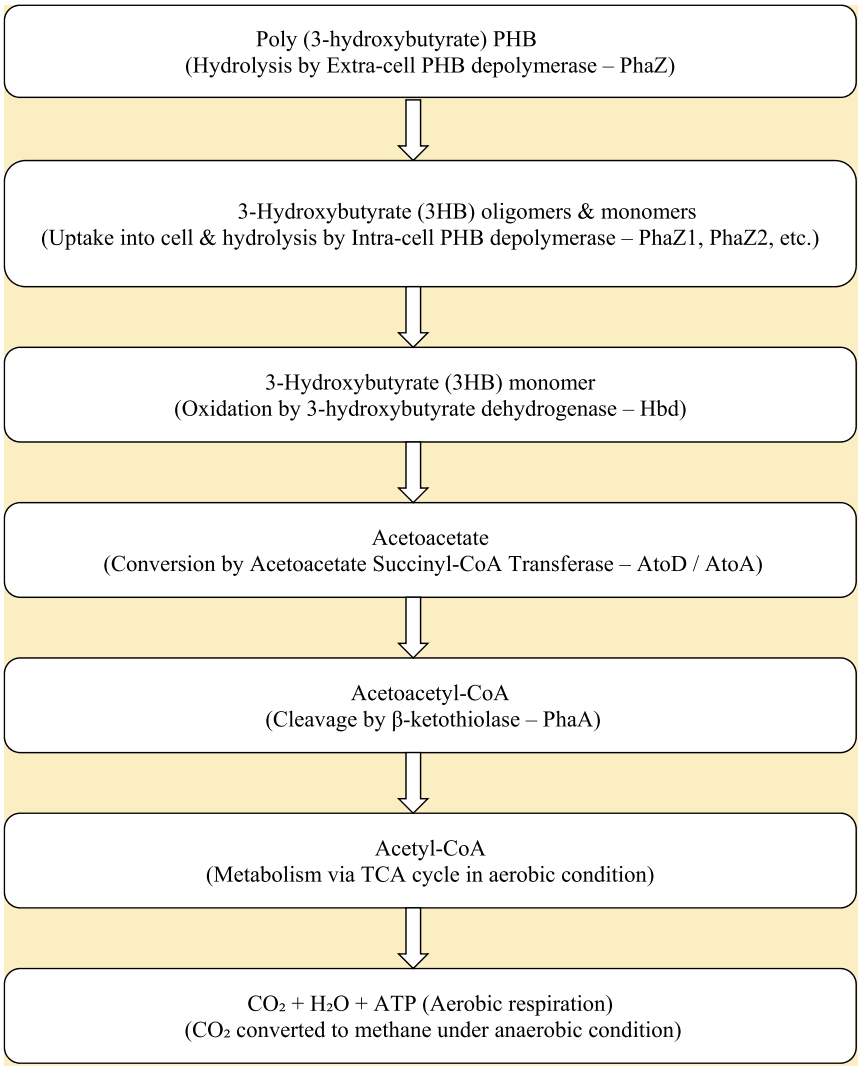

Fig. 10. Metabolic pathway of poly(3-hydroxybutyrate) (PHB) microplastic degradation by PHB depolymerase enzymes under aerobic and anaerobic conditions. This flowchart details the step-wise degradation of PHB microplastics.

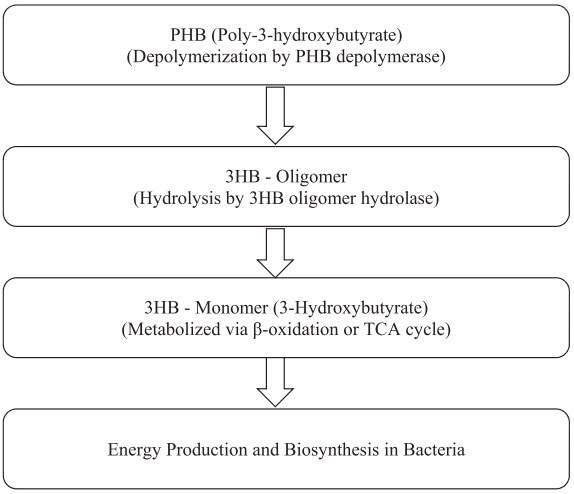

Fig. 11. Metabolic pathway of 3HB-oligomer hydrolase in degrading poly(3-hydroxybutyrate) (PHB) microplastics in bacteria. This flowchart details the step-wise degradation of PHB microplastics.

(Lu et al., 2014; Preetha et al., 2025). All environments contained *Pseudomonas* spp. which reinforces its position as a main degrader of polyhydroxyalkanoates (PHA). Sea samples showed 100 % hit rates of nylon hydrolase and nylon oligomer-degrading enzymes that exist mostly within *Pseudomonas* spp. and *Escherichia coli* which indicates nylon degradation potential is high. The metabolic pathway powered by enzymes nylA, nylB, and nylC utilizes 6-aminohexanoate cyclic dimer hydrolase alongside 6-aminohexanoate oligomer hydrolase and 6-aminohexanoate oligomer endohydrolase to produce adipate from nylon-6 according to documented literature (Takehara et al., 2018). The results from river tests show *Arthrobacter* spp., *Kocuria* spp., and *Flavobacterium* spp. organisms lack the observed enzymes possibly because they possess selective nylon-degrading enzyme activity (Negoro et al., 1992). The alkane hydroxylase-mediated pathway efficiently breaks microplastics such as polystyrene and polyethylene to carboxylic acids which undergo TCA cycle β-oxidation decomposition in river sediment testing *Pseudomonas putida* and *Pseudomonas aeruginosa*. Scientists have already outlined the effective mechanism of plastic degradation through this pathway (Wang et al., 2024a, 2024b). A wide range of plastic materials can be degraded by lipase, protease, esterase, hydrolase, and polyurethanase enzymes which match previously studied plastic degradation activities although their exact pathways remain under investigation (Amobonye et al., 2021). Environmental conditions favour

Table 4
shows the distribution of enzymes with over 50 % activity detected across microplastic samples, as identified by DIAMOND BLAST analysis, irrespective of the presence or identification of known enzyme-producing organisms.

Environment	Enzymes	Samples	Percent hit
Sea Water	3 HV dehydrogenase PHA depolymerase PHB depolymerase Alkane hydroxylase 3HB oligomer hydrolase Nylon -oligomer Degrading enzyme Nylon hydrolase Protease Lipase Esterase Hydrolase	M scale and MM scale microplastic	> 50 %
River	3 HV dehydrogenase PHA depolymerase PHB depolymerase Hydrolase Protease Lipase Esterase 3HB oligomer hydrolase	PLA Water	> 50 %
Soil	3 HV dehydrogenase PHA depolymerase PHB depolymerase Protease Hydrolase Polyurethanase	POM, PP PHA1, POM PHA1, PS PBS, PHA1, POM PS, POM PHA1, POM, PLA, PVC	> 50 %
Anaerobic Sludge	3 HV dehydrogenase PHA depolymerase Protease Lipase Esterase Polyurethanase	PVC	> 50 %

the increased occurrence of 3 HV dehydrogenase in sea and river systems because these aquatic environments contain PHA-like substrates (Mergaert and Swings, 1996). Environmental settings play a decisive role in moulding microbial degradation potentials according to current plastic associated microbiome research (Oberbeckmann and Labrenz, 2020). More significantly researchers confirmed MHETase identification in river environmental samples of PLA and PVC with greater than 98 % sequence homology although taxonomic profiling showed no known MHETase-producing organisms. The enzyme MHETase serves as a vital component for breaking down mono(2-hydroxyethyl) terephthalate which occurs as an intermediate compound during polyethylene terephthalate (PET) hydrolysis especially through bacteria such as *Ideonella sakaiensis* (Yoshida et al., 2016). The strong hit rate indicates that river environments harbour either MHETase-like enzymes or illegible enzymes or genes from unknown or low-population microbial communities. Research demonstrates environmental metagenomes contain MHETase-active polyesterases which appear alongside non-orthodox producers because of gene transfer or evolutionary adaptation processes. The unidentified taxa in our profiling analysis could stem from unsolved taxonomic classification or from microscopic organisms which have not been cultured yet.

A limitation of this study is the lack of metadata on sampling location and seasonality in the retrieved datasets. Although comparisons across environments were conducted, the absence of this contextual information prevents linking observed community differences to geographic or temporal variation.

6. Conclusion

This study demonstrates that microplastic-associated microbial communities exhibit significant taxonomic and functional diversity, with Proteobacteria and Thaumarchaeota dominating across sea, river, soil, and anaerobic sludge environments. Aquatic environments (sea and river) displayed higher species richness and evenness compared to soil, where low diversity and single-species dominance were common. The identification of key plastic-degrading enzymes, such as 3 HV dehydrogenase, PHA depolymerase, PHB depolymerase, nylon hydrolase, and alkane hydroxylase, underscores the biodegradation potential of these communities, particularly for PHA, PHB, and nylon microplastics. Organisms like *Pseudomonas* spp., *Acidovorax* spp., and *Escherichia coli* play pivotal roles in these processes, with their enzymatic activities linked to well-characterized metabolic pathways. The distinct microbial compositions and enzymatic profiles across environments highlight the influence of microplastic type and environmental factors on degradation potential. These findings contribute to our understanding of microbial plastic degradation and provide a foundation for developing targeted bioremediation strategies for microplastic pollution.

CRediT authorship contribution statement

Kavya Sunil: Writing – original draft, Software, Resources, Methodology, Investigation, Formal analysis, Data curation. **Dicky John Davis G:** Writing – review & editing, Validation, Supervision, Project administration, Conceptualization.

Declaration of Generative AI and AI-assisted technologies in the writing process

During the preparation of this work the author(s) used ChatGPT and Grok to improve the clarity and coherence of the manuscript. After using this tool/service, the author(s) reviewed and edited the content as needed and take(s) full responsibility for the content of the published article.

Funding sources

This research did not receive any specific grant from funding agencies in the public, commercial, or not-for-profit sectors.

Declaration of competing interest

The authors declare that we have no competing interest.

Acknowledgement

This study was supported by Galaxy software, which generously provided additional free space upon request, enabling efficient data management and analysis.

Data availability

40 transcriptomic samples were analysed in this study; all sourced from the NCBI-SRA (Sequence Read Archive) database. These data were derived from four distinct types of investigations, each representing different environments, such as Sea water (PRJNA902427), River water (PRJNA714465), Anaerobic sludge (PRJNA1098580), and Soil (PRJNA1146720) from China.

References

Amobonye, A., Bhagwat, P., Singh, S., Pillai, S., 2021. Plastic biodegradation: frontline microbes and their enzymes. Sci. Total Environ. 759, 143536.
Bocci, V., et al., 2024. Freshwater plastisphere: a review on biodiversity, risks, and biodegradation potential with implications for the aquatic ecosystem health. Front. Microbiol. 15, 1395401.
Chen, X., Zhao, Y., Zhou, H., Xiong, X., Wu, C., 2020. Effects of microplastic biofilms on nutrient cycling in simulated freshwater systems. Sci. Total Environ. 719, 137276.
Du, Y., Liu, X., Dong, X., Yin, Z., 2022. A review on marine plastisphere: biodiversity, formation, and role in degradation. Comput. Struct. Biotechnol. J. 20, 975–988.

Galaxy Community, 2024. The Galaxy platform for accessible, reproducible, and collaborative data analyses: 2024 update. Nucleic Acids Res. 52 (W1), W83–W94.
Gupta, A., Gupta, R., Singh, R.L., 2016. Microbes and environment. In: Singh, R.L. (Ed.), Principles and Applications of Environmental Biotechnology for a Sustainable Future. Springer, Singapore, pp. 43–84.
Jacquin, J., Cheng, J., Odobel, C., Pandin, C., Conan, P., Pujo-Pay, M., Barbe, V., Meistertzheim, A.-L., Ghiglione, J.-F., 2019. Microbial ecotoxicology of marine plastic debris: a review on colonization and biodegradation by the "plastisphere". Front. Microbiol. 10, 865.
Jiao, Y., Zhou, A., Zhang, D., Chen, M., Wan, L., 2024. Distinct microbial community structures formed on the biofilms of PLA and PP, influenced by physicochemical factors of sediment and polymer types in a 60-day indoor study. Front. Environ. Sci. 12, 1452523.
Kim, Y., et al., 2024. Biodegradation of poly (butylene adipate terephthalate) and poly (vinyl alcohol) within aquatic pathway. Sci. Total Environ. 953, 176129.
Kumar, G.A., Anjana, K., Hinduja, M., Sujitha, K., Dharani, G., 2020. Review on plastic wastes in marine environment – biodegradation and biotechnological solutions. Mar. Pollut. Bull. 150, 110733.
Lavanya, P., Davis, G.D.J., 2023. Chemo-structural diversity of anti-obesity compound database. J. Mol. Graph. Model. 120, p108414.
Li, C., et al., 2021. The ecology of the plastisphere: Microbial composition, function, assembly, and network in the freshwater and seawater ecosystems. Water Res. 202, 117428.
Li, H.-Q., Wang, W.-L., Shen, Y.-J., Su, J.-Q., 2025. Vegetation, salinity, and tides drive nitrogen cycling in mangrove plastispheres. Sci. Rep. 15, 28792.
Lu, J., Takahashi, A., Ueda, S., 2014. 3-Hydroxybutyrate oligomer hydrolase and 3-hydroxybutyrate dehydrogenase participate in intracellular polyhydroxybutyrate and polyhydroxyvalerate degradation in *Paracoccus denitrificans*. Appl. Environ. Microbiol. 80 (5), 1381–1389.
MacLean, J., Mayanna, S., Benning, L.G., Horn, F., Bartholomäus, A., Wiesner, Y., Wagner, D., Liebner, S., 2021. The terrestrial plastisphere: diversity and polymer-colonizing potential of plastic-associated microbial communities in soil. Microorganisms 9 (9), 1876.
Malla, M.A., Malambule, N.L., Amoah, I.D., Featherston, J., Ismail, A., Bux, F., Kumari, S., 2025. The plastisphere ecology: Assessing the impact of different pollution sources on microbial community composition, function and assembly in aquatic ecosystems. Environmental Chemistry and Ecotoxicology 7, 75–83.
Maran, M.I.J., Davis, G.D.J., 2022. Benefits of merging paired-end reads before pre-processing environmental metagenomics data. Mar. Genomics 61, 100914.
Mergaert, J., Swings, J., 1996. Biodiversity of microorganisms that degrade bacterial and synthetic polyesters. J. Ind. Microbiol. Biotechnol. 17 (6), 463–469.
Mishra, S., et al., 2024. Microplastics-biofilm in aquatic ecosystem: formation, pollutants complexation, greenhouse gas emission and ecotoxicology. J. Environ. Manage. 370, 122930.
Mohanan, N., Montazer, Z., Sharma, P.K., Levin, D.B., 2020. Microbial and enzymatic degradation of synthetic plastics. Front. Microbiol. 11, 580709.
Morohoshi, T., Oi, T., Aiso, H., Suzuki, T., 2018. Biofilm formation and degradation of commercially available biodegradable plastic films by bacterial consortiums in freshwater environments. Microbes Environ. 33 (3), 267–270.
Negoro, S., Kakudo, S., Urabe, I., Okada, H., 1992. A new nylon oligomer degradation gene (nylC) on plasmid pOAD2 from a *Flavobacterium* sp. J. Bacteriol. 174 (24), 7948–7953.
Nguyen, N.H.A., et al., 2023. Early stage biofilm formation on bio-based microplastics in a freshwater reservoir. Sci. Total Environ. 858 (Pt 1), 159569.
Oberbeckmann, S., Labrenz, M., 2020. Marine microbial assemblages on microplastics: diversity, adaptation, and role in degradation. Ann. Rev. Mar. Sci. 12, 209–232.
Oberbeckmann, S., Loeder, M.G.J., Gerdts, G., Osborn, A.M., 2014. Spatial and seasonal variation in diversity and structure of microbial biofilms on marine plastics in Northern European waters. FEMS Microbiol. Ecol. 90 (2), 478–492.
Odobel, C., et al., 2021. Bacterial abundance, diversity and activity during long-term colonization of non-biodegradable and biodegradable plastics in seawater. Front. Microbiol. 12, 734782.
Preetha, R.A., Davis, G.D.J., Neelima, M.G., Chaitra, B.S., Kirankumar, B., 2025. Anti-lipidemic and anti-diabetic properties of *Gymnema sylvestre* saponins: an in-silico approach. In Silico Pharmacol. 13 (2), 94.
Qin, P., et al., 2023. Early stage of biofilm assembly on microplastics is structured by substrate size and bacterial motility. iMeta 2 (3), e121.
Sun, Y., et al., 2022. Biodegradable microplastics enhance soil microbial network complexity and ecological stochasticity. J. Hazard. Mater. 429, 129610.
Sun, X.L., Xiang, H., Xiong, H.Q., Fang, Y.C., Wang, Y., 2023. Bioremediation of microplastics in freshwater environments: a systematic review of biofilm culture, degradation mechanisms, and analytical methods. Sci. Total Environ. 863, 160953.
Takehara, I., et al., 2018. Metabolic pathway of 6-aminohexanoate in the nylon oligomer-degrading bacterium *Arthrobacter* sp. KI72: identification of the enzymes responsible for the conversion of 6-aminohexanoate to adipate. Appl. Microbiol. Biotechnol. 102 (2), 801–814.
Tu, C., et al., 2020. Biofilm formation and its influences on the properties of microplastics as affected by exposure time and depth in the seawater. Sci. Total Environ. 734, 139237.
Vaksmaa, A., et al., 2021. Microbial communities on plastic polymers in the Mediterranean Sea. Front. Microbiol. 12, 673553.
Ventura, E., Marín, A., Gámez-Pérez, J., Cabedo, L., 2024. Recent advances in the relationships between biofilms and microplastics in natural environments. World J. Microbiol. Biotechnol. 40 (7), 220.
Wang, L., et al., 2024a. Soil viral–host interactions regulate microplastic-dependent carbon storage. Proc. Natl. Acad. Sci. U. S. A. 121 (45), e2413245121.
Wang, W., et al., 2024b. Degradation and potential metabolism pathway of polystyrene by bacteria from landfill site. Environ. Pollut. 343, 123202.
Wang, Y., et al., 2025. Degradation of biodegradable plastic films in soil: microplastics formation and soil microbial community dynamics. J. Hazard. Mater. 441, 138250.
Wu, X., Liu, Z., Li, M., Bartlam, M., Wang, Y., 2022. Integrated metagenomic and metatranscriptomic analysis reveals actively expressed antibiotic resistomes in the plastisphere. J. Hazard. Mater. 430, 128418.
Yang, H., Chen, G., Wang, J., 2021. Microplastics in the marine environment: sources, fates, impacts and microbial degradation. Toxics 9 (2), 41.
Yoshida, S., et al., 2016. A bacterium that degrades and assimilates poly (ethylene terephthalate). Science 351 (6278), 1196–1199.
Zahid, H., et al., 2024. Microorganism-mediated biodegradation for effective management and/or removal of micro-plastics from the environment: a comprehensive review. Arch. Microbiol. 206 (4), 198.
Zang, B., Zhou, H., Zhao, Y., Sano, D., Chen, R., 2024. Investigating potential auxiliary anaerobic digestion activity of phage under polyvinyl chloride microplastic stress. J. Hazard. Mater. 479, 135950.
Zettler, E.R., Mincer, T.J., Amaral-Zettler, L.A., 2013. Life in the "plastisphere": microbial communities on plastic marine debris. Environ. Sci. Technol. 47 (13), 7137–7145.
Zhang, S.-J., Zeng, Y.-H., Zhu, J.-M., Cai, Z.-H., Zhou, J., 2022. The structure and assembly mechanisms of plastisphere microbial community in natural marine environment. J. Hazard. Mater. 421, 126780.
Zheng, F., et al., 2024. Urbanization reduces the stability of soil microbial community by reshaping the diversity and network complexity. Chemosphere 343, 143177.